Journal of Porphyrins and Phthalocyanines
J. Porphyrins Phthalocyanines 2019; **23**: 619–627
DOI: 10.1142/S1088424619500299

Published at http://www.worldscinet.com/jpp/

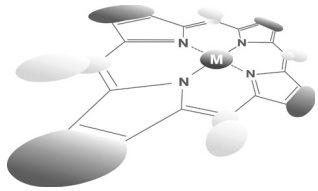

Functionalized Eu(III)-based nanoscale metal-organic framework for enhanced targeted anticancer therapy

Pan Chen, Ya-Fan Huang, Guang-Yu Xu, Jin-Ping Xue and Juan-Juan Chen*

National and Local Joint Biomedical Engineering Research Center on Photodynamic Technologies, and Fujian Engineering Research Center for Drug and Diagnoses and Treatment of Photodynamic Therapy, College of Chemistry, Fuzhou University, Fuzhou, Fujian 350116, China

Received 26 January 2019
Accepted 18 February 2019

ABSTRACT: To improve the cancer targeting and anticancer efficacy, the multifunctional Eu-based metal-organic framework (EuBTC) is post-synthetically modified with a targeting moiety folic acid and a zinc phthalocyanine photosensitizer. In addition, this nanosphere is also applied as a drug delivery system to load the chemical drug doxorubicin. Electron microscopy, powder X-ray diffraction and infrared spectometry demonstrated the formation of these multifunctional nanospheres (DOX). Our nanospheres kept the high singlet oxygen quantum yield of zinc phthalocyanine. Additionally, Cell viability experiments demonstrated the biosafety of EuBTC and the enhanced anticancer effect of DOX@FA-EuBTC-Pc under light irradiation. In short, these well-arranged DOX@FA-Eu-BTC-Pcs exhibit as promising drug delivery systems for enhanced targeted anticancer therapy.

KEYWORDS: photodynamic therapy, combination therapy, metal-organic framework, post-synthetic modification, cancer targeting.

INTRODUCTION

The occurrence and development of malignant tumors is extremely complex. It involves different pathological processes, multiple genes, signal transduction pathways and biological molecular targets [1–2]. Attempts to treat malignant tumors with monotherapeutic approaches are not always efficient. Thus, combination of two treatments with different anticancer mechanisms has been proven to be able to improve the anticancer effect, reducing the rates of metastasis and recurrence, side effects and drug resistance [3–5]. Photodynamic therapy (PDT), a preferred non-invasive therapeutic modality, is approved for a series of tumor diseases [6–7]. The photosensitizers in PDT can be activated to generate reactive oxygen species (ROS) to kill the cancer cells only in the cancer area exposed to light [6–10]. This special ROS-dependent anticancer mechanism makes PDT an ideal cancer therapy to combine with chemotherapy. Combination of PDT and chemical therapy has been demonstrated to improve the anticancer effect [11–13]. However, the photosensitizers are easy to aggregate and poorly targeted. It is greatly desired to create an efficient drug delivery system which can co-load photosensitizers and chemical drugs to maximize the synergistic therapeutic effect and solve the limitation.

Metal-Organic Frameworks (MOFs) have been proven to be extremely valuable materials for their application in catalysis, drug delivery and cancer therapy due to their extra-large surface areas, high pore volumes and flexible structures [14–16]. Furthermore, many multifunctional physicochemical properties of nanomaterials can be achieved through the functionalization of metal-organic frameworks [17–19]. The Eu-based MOFs, especially EuBTC, are very useful carriers due to their unique physicochemical properties such as biocompatibility and a large drug-loading capacity [20–21]. The open metal sites of the central Eu^{3+} endow Eu-N MOFs with a potential functionalized ability through the coordination effect [22–24]. Specifically, EuBTC-NH_2 prepared by organic ligands 2-aminobenzene-1,3,5-tricarboxylic acid can achieve

*Correspondence to: Dr. Juan-Juan Chen, No. 2 Xueyuan Road, College of Chemistry, Fuzhou University, Fuzhou, Fujian 350116, China, tel: +86-591-2286-7963, fax: +86-591-2286-7963, email: cjj_pp@126.com.

chemical modification more easily by the post-synthetic modifications. Therefore, we hope to apply the EuBTC nanosystem to become a multi-functional platform for co-delivery of photosensitizers and chemical drugs to enhance the anticancer activities, and to immobilize targeting ligands to improve cancer targeting.

In this study, we first anchor zinc phthalocyanines (ZnPc), excellent photosensitizers with good singlet oxygen production [25–28], on the surface of EuBTC *via* amidation to avoid aggregation; less aggregation will result in higher singlet oxygen generation. Second, we decorate EuBTC-NH2 with folic acid (FA), which can target the highly expressed FA acceptor in cancer cells likes epithelial, ovarian, cervical, breast, lung, kidney, colorectal and brain tumors [29–31]. Finally, a well-known chemical drug, doxorubicin (DOX) [32–34], is loaded into the nanosystem. Therefore, we synthesized a multifunctional platform named DOX@FA-EuBTC-Pc (Scheme 1) to improve cancer targeting and anticancer efficacy.

RESULTS AND DISCUSSION

Synthesis

As shown in Scheme 1 and Schemes S1–S2 and Figs S1–S6 (see supporting information) the EuBTC-NH_2 was prepared *via* a solvothermal reaction of $Eu(NO_3)_3 \cdot 6H_2O$, BTC-NH_2 in *N*,*N* dimethyl formamide. Polyvinyl pyrrolidone (PVP) and sodium acetate were added to modulate the size of the nanoparticles. Then, a covalent post-synthetic method was used to achieve FA-EuBTC-Pc powders through chemical modification of EuBTC-NH_2 by amidation reaction with **ZnPc-TCP** and folic acid. The powders remain blue colored after washing by DMF and ethanol, which indicates the presence of **ZnPc-TCP**. **ZnPc-TCP** and folic acid are on the surface of EuBTC-NH_2 nanoparticles after the amidation reaction and are expected to keep their photosensitivity and cancer targeting abilities. Finally, DOX was loaded into the nanoparticles. The encapsulation efficiency was 41.48% and the loading capacity was 41.66% as determined by UV-vis spectrometry. DOX@FA-EuBTC-Pc NPs was confirmed with high drug-loading and encapsulation efficiency.

Characterization

The scanning electron microscopy images in Fig. 1 show that EuBTC is shaped like a claviform raisin with a diameter of about 200 nm. However, EuBTC-NH_2 became spheres or short rods with much smaller size (20–50 nm) than that of EuBTC because of the coordination of the amino group and Eu^{3+}. The morphology of the nanoparticles also changed after modification by **ZnPc-TCP**. The morphology is consistent with that previously

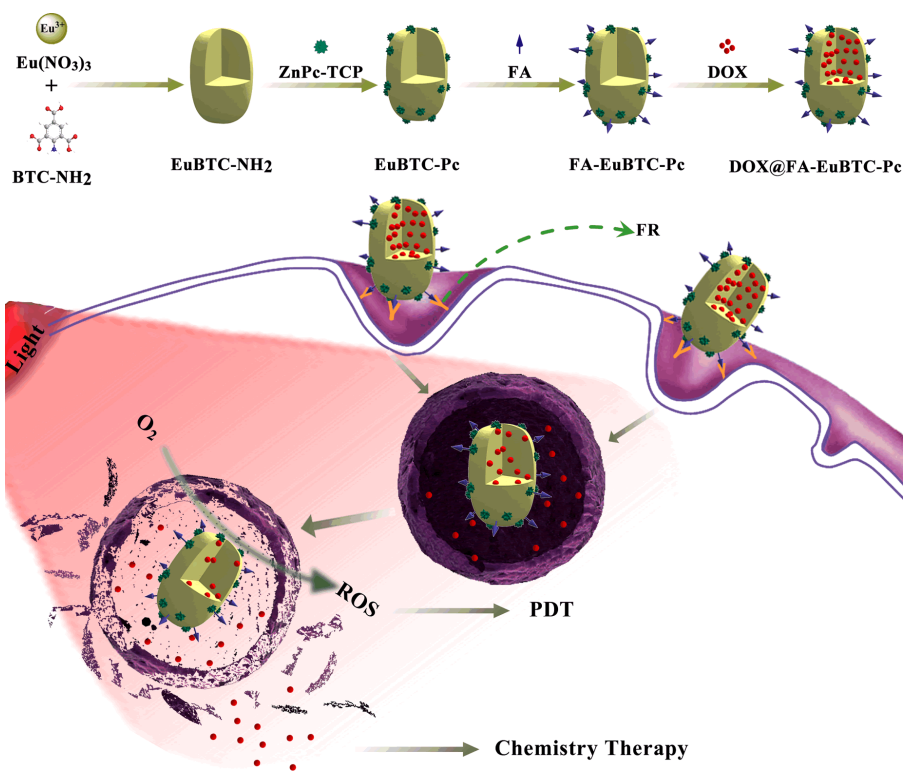

Scheme 1. Schematic illustration of the structure and assembly route of the DOX@FA-EuBTC-Pc NPs, and the mechanism of DOX@FA-EuBTC-Pc NPs at tumor site including 670 nm light irradiation in tumor, ROS production, and DOX release for synergistical anticancer effect. BTC-NH_2 = 2-amino-1,3,5-benzenetricarboxylic acid, Pc = tetrakis(4-carboxylphenoxy) phthalocyanine zinc, FA = folic acid, DOX = doxorubicin

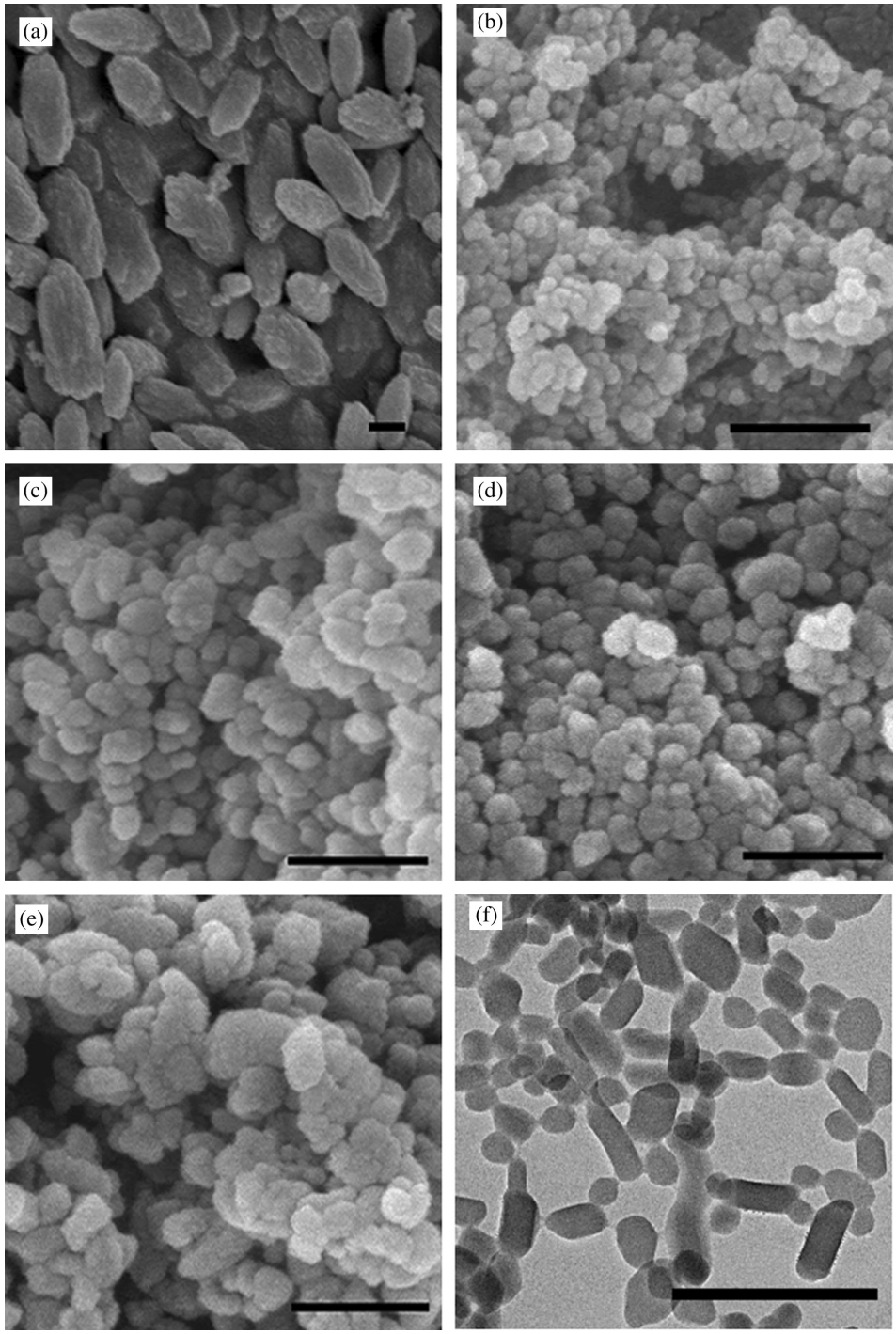

Fig. 1. SEM of (a) EuBTC, (b) EuBTC-NH_2, (c) EuBTC-Pc, (d) FA-EuBTC-Pc and (e) DOX@FA-EuBTC-Pc; (f) TEM of DOX@FA-EuBTC-Pc. Bar = 200 nm

observed with the size almost unchanged. With the load of DOX, the nanoparticle size becomes larger. Further, these results were confirmed correspondingly by DLS (Fig. S7).

Powder X-ray diffraction (PXRD) of the EuBTC nanoparticles is shown in Fig. 2a. The well-defined diffraction peaks of all nanoparticles indicate that these nanoparticles have high crystallinity, in accordance with that of the simulated EuBTC. The post-synthetic modification reaction of EuBTC-NH_2 was also confirmed by FT-IR spectroscopy. As shown in Fig. 2b, the characteristic double peak of the amino groups is obviously visible near 3317 cm^{-1} and 3303 cm^{-1} (N–H stretching vibration) in the FT-IR spectra of EuBTC-NH_2. After modification with phthalocyanine, the characteristic peak of the amino group was nearly disappeared, and a tip peak at 3431 cm^{-1} was generated, which indicates the stretching vibration of RCON-HR. At the same time, the amino group was not completely reacted, so there is still a weak peak at

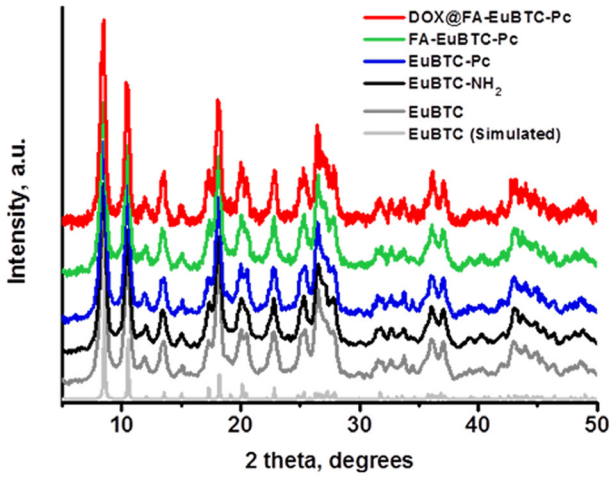

(a)

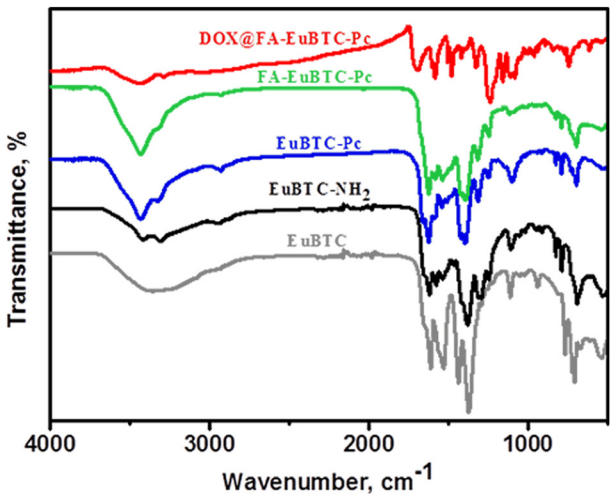

(b)

Fig. 2. (a) XRD patterns of EuBTC, EuBTC-NH_2, EuBTC-Pc, FA-EuBTC-Pc, and DOX@FA-EuBTC-Pc. (b) IR spectra of EuBTC, EuBTC-NH_2, EuBTC-Pc, FA-EuBTC-Pc, and DOX@FA-EuBTC-Pc

3310 cm^{-1}. With conjugation to folic acid, the characteristic stretching vibration peak of the amino group basically disappeared, and only one sharp peak at 3431 cm^{-1} remains.

Singlet oxygen quantum yield

Singlet oxygen is the key effect factor in photodynamic anticancer therapy. To determine the singlet oxygen quantum yield, we used the singlet oxygen trapping agent 1,3-diphenylisobenzofuran (DPBF). The change of its absorbance value at 415 nm in all NPs and **ZnPc-TCP** solution was recorded by UV-vis photometry (Fig. 3). The singlet quantum yields (Φ_Δ) of all nanoparticles and **ZnPc-TCP** are shown in Table 1. All nanoparticles have almost the same singlet quantum yields (0.53–0.59) as that of **ZnPc-TCP**, which indicates that all the nanoparticles retain the high photosensitivity of **ZnPc-TCP**.

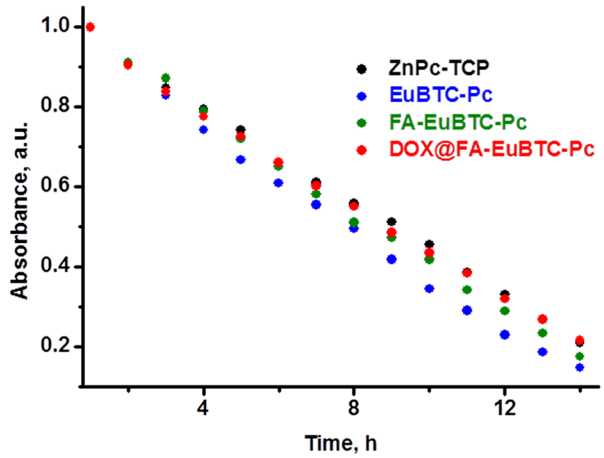

Fig. 3. The UV-vis absorbance change of DPBF at 415 nm in **ZnPc-TCP** and all NPs solution

Drug release

We suspect that DOX is not simply adsorbed in the carrier channel of EuBTC, but is coordinated with the remaining Eu ion sites, and the strength of coordination is affected by pH. The pH value of cancer tissues and cells is 5.0–6.0, which is lower than that of blood and normal tissues (pH = 7.4). Therefore, the release of DOX from DOX@FA-EuBTC-Pc was analyzed by membrane dialysis in phosphate-buffered saline with different pH (Fig. 4). We use pH = 5.0 and 6.0 to mimic the cancer tissues and cells, and pH = 7.4 for bloodstream and normal tissues. Less than 12% of DOX was released at pH 7.4. By comparison, markedly increased release rates and amounts were observed when the pH was lowered to 6.0 and 5.0. More than 60% of DOX released around 8 h and the drug release content within 24 h was nearly to 80% at pH 5.0. This result demonstrates that DOX@FA-EuBTC-Pc can only release DOX in cancer cells and not leak into the blood and normal tissues.

Cellular uptake and subcellular localization

To verify the cancer-targeting properties of the nanoparticles, a relative cellular uptake experiment was

Table 1. Φ_Δ of **ZnPc-TCP** and all NPs obtained by chemical quenching of DPBF at 415 nm

Compound	**ZnPc-TCP**	EuBTC-Pc	FA-EuBTC-Pc	DOX@FA-EuBTC-Pc
Φ_Δ	0.54	0.59	0.57	0.53

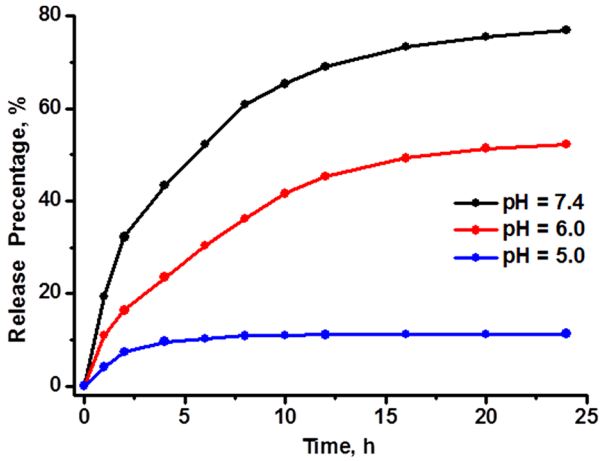

Fig. 4. Release curve of DOX from DOX@FA-EuBTC-Pc nanoparticles in the different pH PBS

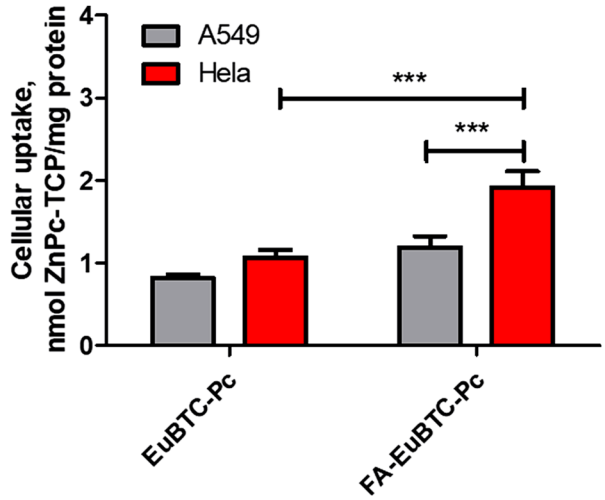

Fig. 5. Cellular uptake of EuBTC-Pc and FA-EuBTC-Pc at 10 μM in A549 cells and HeLa cells (***$p < 0.001$)

performed (Fig. 5). We choose HeLa cells with high expressions of FA receptors and A549 cells with low expressions of FA receptors. As expected, the cellular uptake of FA-EuBTC-Pc in HeLa cells is much higher than that in A549 cells with significant difference. A significant difference between the uptake of FA-EuBTC-Pc and EuBTC-Pc can also be found. However, there is no obvious difference between the cellular uptake of EuBTC-Pc, which has no FA moieties, in HeLa cells and A549 cells. The result indicates that the introduction of folic acid targeting groups can improve cancer targeting, and then significantly increase the cellular uptake in high FR-receptor-expression cancer cells.

In order to demonstrate that FA-EuBTC-Pc can target the FA receptor and then be endocytosed and localized in lysosomes, we used confocal laser scanning microscopy to study subcellular lolization. As shown in Fig. 6, the

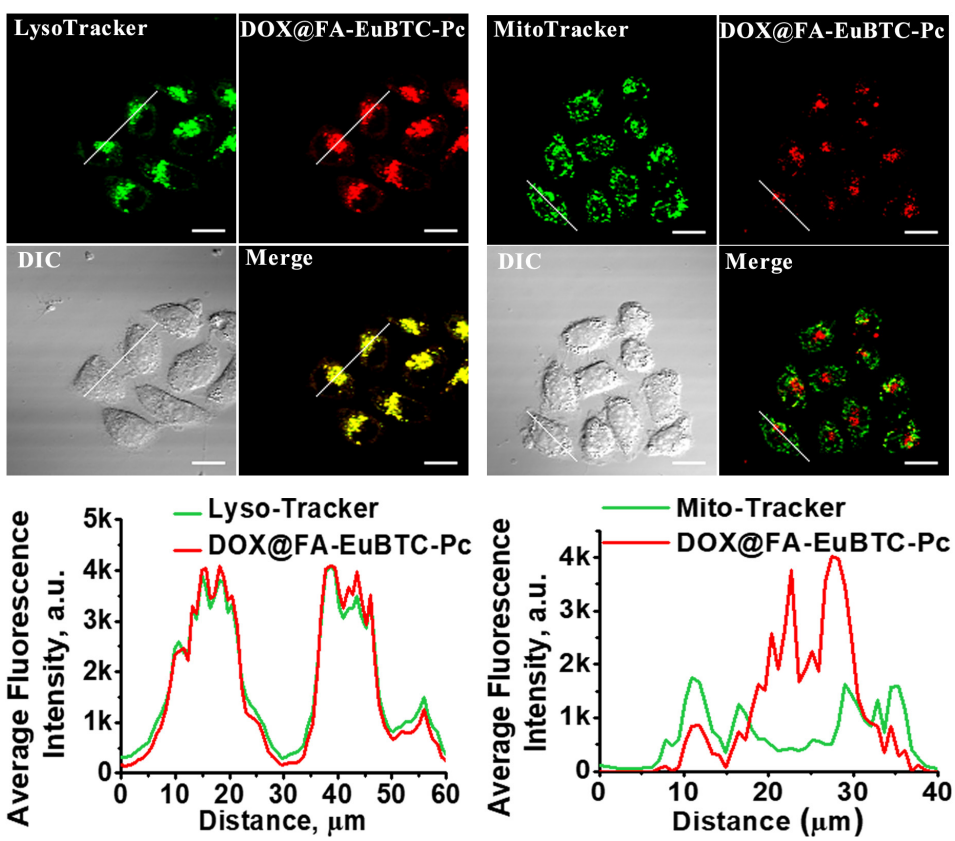

Fig. 6. Confocal laser scanning microscopy images of HeLa cells incubated with FA-EuBTC-Pc for 24 h

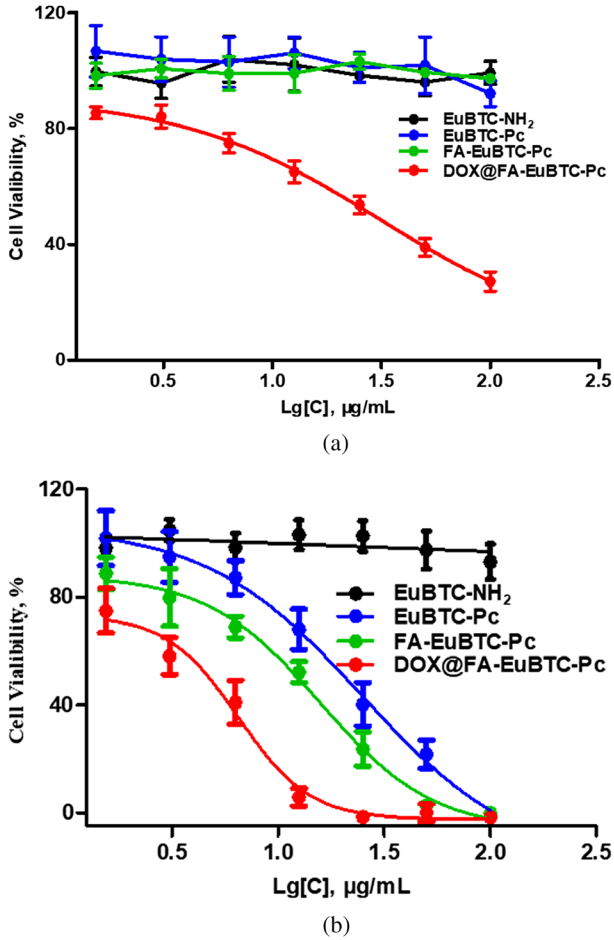

Fig. 7. Cytotoxic effects of EuBTC-NH_2, EuBTC-Pc, FA-EuBTC-Pc, and DOX@FA-EuBTC-Pc NPs towards HeLa cells in (a) dark and (b) light irradiation

fluorescence images of lysosomes were overlapped well with that of FA-EuBTC-Pc, which means good colocalization. There is almost no colocalization between mitochondria and FA-EuBTC-Pc. Therefore, FA-EuBTC-Pc can enter into cancer cells by FA receptor-mediated endocytosis and be mainly distributed in the lysosomes.

Cytotoxicity experiment

To study the anticancer effect of all nanoparticles, a 3-(4,5-dimethyl-2-thiazolyl)-2,5-diphenyl-2H-tetrazolium bromide (MTT) cell viability assay was used to detected the half-maximum inhibitory concentration value (IC_{50}) values. In Fig. 7 there was nearly no cytotoxicity of other nanoparticles in the dark condition, except for DOX@FA-EuBTC-Pc, which has chemical toxicity because of DOX. The result indicates that EuBTC-NH_2, EuBTC-Pc, FA-EuBTC-Pc are biocompatible and non-cytotoxic in dark. After 670 nm irradiation, EuBTC-NH_2 still showed no obvious cytotoxicity towards HeLa cells, suggesting that EuBTC is also biosafe under light

Table 2. IC_{50} values of EuBTC-NH_2, EuBTC-Pc, FA-EuBTC-Pc, and DOX@FA-EuBTC-Pc towards HeLa cells

Nanoparticles	IC_{50} (μg/mL)	
	Dark	Light
EuBTC-NH_2	>100	>100
EuBTC-Pc	>100	24.91
FA-EuBTC-Pc	>100	15.79
DOX@FA-EuBTC-Pc	31.51	6.508

irradiation. EuBTC-Pc, FA-EuBTC-Pc and DOX@FA-EuBTC-Pc all showed significant phototoxicity. According to the cytotoxicity curve, we can obtain the IC_{50} values and the results are shown in Table 2. The IC_{50} values of EuBTC-Pc, FA-EuBTC-Pc and DOX@FA-EuBTC-Pc were 24.91 ug/mL, 15.79 ug/mL, 6.508 ug/mL, respectively. Because of FA cancer targeting, increased uptake of FA-EuBTC-Pc makes it more cytotoxic. The anticancer ability of DOX@FA-EuBTC-Pc has been greatly improved by combination of DOX and **ZnPc-TCP**. The results indicate that the synergistic anticancer effect of photosensitizers and DOX in this nanosystem and the introduction of folic acid improve cytotoxicity towards cancer cells because of cancer targeting.

EXPERIMENTAL

Materials and methods

All reagents and solvents were obtained from commercial sources (Alfa Aesar, Sigma-Aldrich, Aladdin) and used without further purification.

The morphology of the sample was investigated by field emission scanning electron microscopy (SEM) (Hitachi S4800, Tokyo, Japan). TEM images were taken on a high-resolution transmission electron microscope (HR-TEM, Tecnai G2 F20 S-TWIN, 200 kV, FEI Company, USA) operated at an acceleration voltage of 200 keV by dropping solution onto a carbon-coated copper grid. Powder X-ray diffraction (PXRD) was carried out on a Bruker D8-Focus Bragg–Brentano X-ray Powder Diffractometer equipped with Cu Ka1 radiation (k = 1.5406 Å). X-ray photoelectron spectroscopy (XPS) data were obtained on Thermo ESCALAB250 instrument with a monochromatized Al Kα line source (200 W). Fourier transformed infrared (FTIR) spectra were recorded on BioRad FTS 6000 spectrometer using KBr pellet in 400–4000 cm^{-1} range. UV-vis spectra were recorded on Beijing PuXi Tu-1901 spectrophotometer. Fluorescence spectra were recorded on a Varian Cary Eclipse spectrometer with a Xe lamp as the excitation

source at room temperature. The singlet oxygen quantum yields were determined a UV-vis spectrophotometer (TU-1901). The fluorescence intensity of zinc phthalocyanine in the cells was monitored by flow cytometry (C6, BD BioSciences). Cell Counting Kit-8 (CCK-8) was obtained from Beyotime Institute of Biotechnology. Confocal laser scanning microscopy (CLSM) images were performed on an Olympus FV1000-IX81 CLSM and a Leica TCS SP confocal system (Leica, Germany).

Synthesis

***Preparation of tetrakis* (4-*carboxylphenoxy*) *phthalocyanine zinc* (*ZnPc-TCP*).** **ZnPc-TCP** was carried out under conditions reported by Ke *et al.* [35] using 3-nitrophthalonitrile, 4-(butoxycarbonyl) phenol and anhydrous K_2CO_3 in dry DMSO, followed by filtration and washing. Zinc acetate and DBU were reacted with the above procedure, finally followed by hydrolysis. Compound **ZnPc-TCP** was obtained as a green solid (Yield 22.5%). ^{1}H NMR (400 MHz, DMSO) δ9.00 (s, 2H), 8.38 (d, J = 22.0 Hz, 2H), 7.92 (d, J = 37.5 Hz, 14H), 7.29 (d, J = 63.3 Hz, 10H). MS (ESI): (*m/z*) 1121.1473 {80%, $[M + H]^+$}.

Preparation of* 2-*amino*-1,3,5-*benzenetricarboxylic acid. Synthesis of 2-aminotrimethylenetricarboxylic acid ligands was carried out under conditions reported by Peikert *et al.* [36], with some improvements.

***Preparation of trimethyl* 2-*bromobenzene*-1,3,5-*tricarboxylate* (*Y2*).** 5 g (25 mmol) of 2-bromo-1,3,5-trimethylbenzene and 300 mL of boiling water were mixed and stirred for 10 min, 26 g (0.16 mol) of potassium permanganate added, and then all mixtures were heated to reflux. After 72 h, 50 mL of methanol was added, and the reaction was stirred at 60 °C for 5 h to remove unreacted potassium permanganate. Next, the mixture was filtered and washed with boiling water, then the collected filtrate was removed by rotary evaporation and acidified to pH = 1 with 50% sulfuric acid. The white powder was precipitated to obtain a solid powder of 3.4 g 2-bromobenzene-1,3,5-tricarboxylic acid. 3 g (10.4 mmol) of 2-bromobenzene-1,3,5-tricarboxylic acid was dissolved in 60 mL methanol, and 3 mL concentrated sulfuric acid was added dropwise. The mixture was heated under reflux for 6 h, and then was poured into ice water. The pH was adjusted to neutral with saturated sodium hydrogen carbonate, and the precipitate was collected by filtration to yield 1.8 g of white powder. ^{1}H NMR (400 MHz, $CDCl_3$) δ8.35 (s, 2H), 3.98 (s, 6H), 3.96 (s, 3H).

***Preparation of trimethyl* 2-(*benzylamino*)*benzene*-1,3,5-*tricarboxylate* (*Y3*).** 2 g (6.1 mmol) of **Y2** was dissolved in a mixed solution of 30 mL of methanol, 15 mL of dioxane, and 4.5 mL of benzylamine, and stirred at room temperature for 10 min, then transferred to an oven at 40 °C for 4 h. After the reaction was completed, the solvent was spun off, 50 mL of water was added, and the precipitate was acidified by adding 1 M of dilute hydrochloric acid to collect a solid to obtain 1.6 g white powder. ^{1}H NMR (400 MHz, $CDCl_3$) δ 8.56 (s, 2H), 7.36–7.27 (m, 5H), 4.28 (s, 2H), 3.89 (s, 3H), 3.87 (s, 6H).

***Preparation of Trimethyl* 2-*aminobenzene*-1,3,5-*tricarboxylate* (*Y4*).** 2 g (5.6 mmol) of **Y3**, 0.56 g of Pd/C was dissolved in a mixed solution of 65 mL of tetrahydrofuran and 20 mL of isopropanol and reacted at room temperature for 2 days under a hydrogen atmosphere. After the reaction was completed, the mixture was filtered through celite and washed with dichloromethane. The filtrate was spun dry to obtain 1.25 g white powder. ^{1}H NMR (400 MHz, $CDCl_3$) δ8.76 (s, 2H), 8.60 (s, 2H), 3.91 (s, 6H), 3.90 (s, 3H).

***Preparation of* 2-*aminobenzene*-1,3,5-*tricarboxylic acid* (*Y5*).** 3 g (11.2 mmol) of **Y4** was dissolved in 50 mL of tetrahydrofuran and 100 ml of water, and 30 mL of a 2 M KOH solution was added, and the mixture was heated to 50 °C overnight. After the reaction was completed, the organic solvent was removed and the aqueous phase was acidified with dilute hydrochloric acid to give a white powder (2.1 g). ^{1}H NMR (400 MHz, $CDCl_3$) δ13.06 (s, 3H), 8.61 (s, 2H), 8.58 (s, 2H).

Preparation of EuBTC-NH$_2$. The precursor solution 60 mg (0.135 mmol) $Eu(NO_3)_3 \cdot 6H_2O$, 20 mg (0.090 mmol) **Y5** and DMF (3 mL) were placed in a centrifuge tube. Then 0.73 g polyvinyl pyrrolidone (PVP) and 24.6 mg sodium acetate were dissolved in a mixed solution containing DMF (3 mL), ethanol (4 mL) and H_2O (4 mL). The precursor solution was added to the mixed solution. Next, the final solution was shifted to a glass vial and heated to 120 °C for 18 h. The precipitates were washed with DMF three times, ethanol two times, then the sample powder was dried under vacuum and a pale yellow powder was obtained.

Preparation of EuBTC-Pc. 20 mg **ZnPc-TCP** was dissolved in 4 mL DMF and 8.5 mg (0.05 mmol) 1-ethyl-3-(3-dimethylaminopropyl) carbodiimide (EDCI) and 6.0 mg (0.05 mmol) 1-hydroxybenzotriazole (HOBT) was added. The mixed solution was kept stirring at 0 °C for about 30 min. Then 5 drops of triethylamine were added to maintained the system pH at 7–8. Next, 20 mg EuBTC-NH_2 was added and stirred overnight when the temperature was raised to room temperature. After the reaction, the sample was collected by centrifugation, washed with DMF and ethanol. The sample was dried under vacuum and a blue powder was obtained.

Preparation of FA-EuBTC-Pc. 35.0 mg (0.08 mmol) FA was dissolved in a water-DMSO mixture (1:1v/v, 8 mL), and 0.2 mL triethylamine was added to keep the pH at about 8. Then 32 mg (0.17 mmol) 1-Ethyl-3-(3′-dimethylaminopropyl) carbodimi-de (EDC) and 18 mg (0.16 mmol) *N*-Hydroxysuccinimide (NHS) were added. The mixture was stirred for 4 h at room temperature under dark conditions. After 4 h, 20 mg EuBTC-Pc was added to the FA solution and the mixture was stirred for 24 h under dark. The sample was washed with H_2O and

ethanol. The sample was dried under vacuum and a pale blue powder was obtained.

Preparation of DOX@FA-EuBTC-Pc. 16 mg DOX was dissolved in 4 mL water and 20 mg FA-Eu-BTC-Pc was added. The mixture was stirred for 24 h. After 24 h, the powder was isolated by centrifugation, washed several times with H_2O and ethanol and dried in a vacuum.

Singlet oxygen quantum yields

The photosensitizing efficiencies of **ZnPc-TCP**, EuBTC-Pc, FA-EuBTC-Pc, and DOX@FA-EuBTC-Pc were investigated using 1,3-diphenylisobenzofuran (DPBF) as the singlet oxygen sweeper agent to test their singlet oxygen quantum yields in DMF. The oxygen-saturated DMF solution (3 mL) of DPBF (25 mM) was mixed with **ZnPc-TCP** (about 0.1 mmol, the same for NPs for 0.4 mg) in a cuvette. A 670 nm light source was used and the typical zinc(II) phthalocyanine (ZnPc) was selected as the standard with a value for singlet oxygen quantum yields std = 0.56. 670 nm light was irradiated 60 s and the change of the absorbance value at 415 nm was recorded by UV-vis photometers.

Drug loading and release

16 mg of DOX and 20 mg of FA-EuBTC-Pc NPs were dissolved in a mixture of H_2O and mixed by a magnetic stirrer at room temperature for 2 h. Next the mixture was centrifuged at 3000 × g for 5 min to separate the unloaded material from nanoparticles, and then this step was repeated 3 times. DOX@FA-EuBTC-Pc NPs were quantified using a UV-vis spectrophotometer at 497 nm. The encapsulation efficiency was determined by a suitable amount supernatant of DOX@FA-EuBTC-Pc NPs in 3 mL H_2O and was analyzed by the UV-vis spectrophotometry. The drug-loading content was also analyzed by the UV-vis spectra and analytical balances.

For *in vitro* release of DOX from nanospheres, 10 mg of DOX@FA-EuBTC-Pc NPs was placed in a dialysis bag (Mw cutoff of 1000 Da), then suspended in different beakers containing 50 mL of different pH PBS (0.01 M, pH 5.0, pH 6.0, pH 7.4) and mixed by a magnetic stirrer at 37 °C. At 0, 1, 4, 6, 8, 10, 12, 16, 20, 24 h, a sample of 3 mL was withdrawn from the beaker and taken the place of the same amount of fresh release medium. Next, the sample was analyzed by UV-vis spectometry and the real-time absorbance of DOX was calculated.

Cellular uptake

A549 and HeLa cells were plated at 60,000 cells per well in 96-well plates and 6 duplicate holes were set. EuBTC-Pc and FA-EuBTC-Pc stock solutions in water containing 5% Tween (10 mg/mL) were diluted to give 100 ug/mL in medium (the final DMSO concentration was 1% in medium). The old medium was discarded and the above mixed solution was added into the plate. After incubation for 24 h, the medium was removed and washed three times with PBS, then the cells were lysed with 2% SDS (200 uL) for 2 h to give a homogenous solution. The fluorescence of the cell extract was then measured on a Bio-Tek microplate reader at 562 nm. We used the BCA protein method to get the corresponding cell number data.

Confocal microscopy

Approximately 60 000 HeLa cells in the culture medium (1 mL) were plated on a culture dish and incubated for 24 h. Then, the medium was replaced by a fresh medium with FA-EuBTC-Pc and incubated for another 24 h. After incubation, the cells were rinsed with physiological saline and incubated with 75 nM LysoTracker Green, 50 nM Mito-Tracker Green for 30 min, or 1 ug/mL DAPI for 5 min. Then corresponding fluorescence images were taken.

Cytotoxicity assay

HeLa cells were seeded onto 96-well plates at 60,000 cells per well and incubated overnight. EuBTC-NH_2, EuBTC-Pc, FA-EuBTC-Pc and DOX@FA-EuBTC-Pc NPs were diluted to the needed concentration and added to six plicate wells. After 24 h incubation, the media containing drugs were replaced by fresh media and the cells were exposed to a light dose of 2 J/cm^2. After irradiation, the cells were incubated again for 24 h, and then 10 uL MTT solution was added to each well followed by incubation for 4 h. 100 uL DMSO was then added into each well. The plate was incubated at room temperature for 20 min. The absorbance at 570 nm of each well was measured by a microplate reader. For dark toxicity, the procedures were almost the same as above, expect that there was no irradiation.

CONCLUSION

In summary, we have fabricated and fully characterized DOX@FA-EuBTC-Pc nanoparticles *via* post-synthetic modification. These nanoparticles show high singlet oxygen generation and DOX release efficiency, good cancer targeting and enhanced anticancer activity. Therefore, the DOX@FA-EuBTC-Pc nanosystem is a promising agent for cancer therapy. It is hoped that our work can provide a novel method for the design and preparation of MOFs for targeted combination therapy, which may offer more elicitation for MOFs in cancer treatment applications.

Acknowledgments

This work was supported by the National Natural Science Foundation of China (No. 81703345 and

51672046) and the National Health and Family Planning Commission jointly established a scientific research fund (Project No. WKJ2016-2-14).

Supporting information

Schemes S1–S2 and Figures S1–S7 are given in the supplementary material. This material is available free of charge *via* the Internet at http://www.worldscinet.com/jpp/jpp.shtml.

REFERENCES

1. Cao Y, Li Y, Hu X-Y, Zou X, Xiong S, Lin C and Wang L. *Chem. Mater.* 2016; **27**: 1110–1119.
2. Mingbin Z, Caixia Y, Yifan M, Ping G, Pengfei Z, Cuifang Z, Zonghai S, Pengfei Z, Zhaohui W and Lintao C. *ACS Nano* 2013; **7**: 2056–2067.
3. Feril L-B Jr, Kondo T, Umemura SI, Tachibana K, Manalo AH and Riesz P. *J. Med. Ultrason.* 2002; **29**: 173–187.
4. Zhang D, Wu M, Zeng Y, Wu L, Wang Q, Han X, Liu X and Liu J. *ACS. Appl. Mater. Inter.* 2015; **7**: 8176–8187.
5. Barbosa S, Topete A, Alatorre-Meda M, Villar-Alvarez E-M, Pardo A, Alvarez-Lorenzo C, Concheiro A, Taboada P and Mosquera V. *J. Phys. Chem. C* 2014; **118**: 26313–26323.
6. Baptista MS, Cadet J, Di Mascio P, Ghogare AA, Greer A, Hamblin MR, Lorente C, Nunez SC, Ribeiro MS, Thomas AH, Vignoni M and Yoshimura TM. *Photochem. Photobiol.* 2017; **93**: 912–919.
7. Wainwright M. *Anti-Cancer Agents Med. Chem.* 2008; **8**: 280–291.
8. Celli JP, Spring BQ, Rizvi I, Evans CL, Samkoe KS, Verma S, Pogue BW and Hasan T. *Chem. Rev.* 2010; **110**: 2795–2838.
9. Jori G, Fabris C, Soncin M, Ferro S, Coppellotti O, Dei D, Fantetti L, Chiti G and Roncucci G. *Lasers Surg. Med.* 2006; **38**: 468–481.
10. Juarranz A, Jaen P, Sanz-Rodriguez F, Cuevas J and Gonzalez S. *Clin. Transl. Oncol.* 2008; **10**: 148–154.
11. Hornung R, Walt H, Crompton NE, Keefe KA, Jentsch B, Perewusnyk G, Haller U and Köchli OR. *Photochem. Photobiol.* 2010; **68**: 569–574.
12. Kimura M, Miyajima K, Kojika M, Kono T and Kato H. *Int. J. Mol. Sci.* 2015; **16**: 25466–25475.
13. Zhang D, Zheng A, Li J, Wu M, Cai Z, Wu L, Wei Z, Yang H, Liu X and Liu J. *Adv. Sci.* 2017; **4**: 1600460/1–1600460/9.
14. Lismont M, Dreesen L and Wuttke S. *Adv. Funct. Mater.* 2017; **27**: 1606314/1–1606314/16.
15. Nian F, Huang Y, Song M, Chen J-J and Xue J. *J. Mater. Chem. B* 2017; **5**: 6227–6232.
16. Wang C, Liu D and Lin W. *J. Am. Chem. Soc.* 2013; **135**: 13222–13234.
17. Tranchemontagne DJ, Hunt JR and Yaghi OM. *Tetrahedron* 2008; **64**: 8553–8557.
18. Whitfield TR, Wang XQ, Liu LM and Jacobson AJ. *Solid State Sci.* 2005; **7**: 1096–1103.
19. Horcajada P, Serre C, Maurin G, Ramsahye NA, Balas F, Vallet-Regi M, Sebban M, Taulelle F and Ferey G. *J. Am. Chem. Soc*. 2008; **130**: 6774–6780.
20. Jia J, Zhang Y, Zheng M, Shan C, Yan H, Wu W, Gao X, Cheng B, Liu W and Tang Y. *Inorg Chem.* 2017; **57**: 300–310.
21. Xu B, Guo H, Song W, Li Y, Zhang H and Liu C. *CrystEngComm*. 2012; **14**: 2914–2919.
22. Elgundi Z, Reslan M, Cruz E, Sifniotis V and Kayser V. *Adv. Drug Deliver. Rev.* 2017; **122**: 2–19.
23. Dosio F, Arpicco S, Stella B and Fattal E. *Adv. Drug Deliver. Rev.* 2016; **97**: 204–236.
24. Campbell WM, Burrell AK, Officer DL and Jolley KW. *Coord. Chem. Rev.* 2004; **248**: 1363–1379.
25. O'Connor AE, Gallagher WM and Byrne AT. *Photochem. Photobiol.* 2009; **85**: 1053–1074.
26. Collman JP, Gagne RR, Reed CA, Halbert TR, Lang G and Robinson WT. *J. Am. Chem. Soc.* 1975; **97**: 1427–1439.
27. Moan J and Berg K. *Photochem. Photobiol.* 2010; **53**: 549–553.
28. Elemans JAAW, *van* Hameren R, Nolte RJM and Rowan AE. *Adv. Mater.* 2010; **18**: 1251–1266.
29. Brouwer DA, Welten HT, Reijngoud DJ, van Doormaal JJ and Muskiet FA. *Clin. Chem.* 1998; **44**: 1545–1550.
30. Fife J, Raniga S, Hider PN and Frizelle FA. *Colorectal. Dis.* 2011; **13**: 132–137.
31. Wei S, Zhao F, Xu Z and Zeng B. *Microchim. Acta*. 2006; **152**: 285–290.
32. Reck M, Krzakowski M, Jassem J, Eschbach C, Kozielski J, Costanzi JJ, Gatzemeier UK Shogen and Von PJ. *J. Clin. Oncol.* 2009; **27**: 7507–7507.
33. Ogawara KI, Un K, Tanaka KI, Higaki K and Kimura T. *J. Controlled Release* 2009; **133**: 4–10.
34. Du H, Cui C, Wang L, Liu H and Cui G. *Mol. Pharm.* 2011; **8**: 1224–1232.
35. Ke M-R, Huang J-D and Weng S-M. *J. Photochem Photobiol. A* 2009; **201**: 23–31.
36. Peikert K, Hoffmann F and Froba M. *Chem. Commun.* 2012; **48**: 11196–11198.